  Bull. Chem. Soc. Jpn., 60, 193—200 (1987)

Thermal Condensation in Solid State of *N*-Hydroxyalkyl-2-imidazolidinone

Choichiro SHIMASAKI,* Ryosei KANAYAMA, Hiroaki YOSHIDA, and Makoto YUGAMIDANI
Faculty of Engineering, Toyama University, Gofuku, Toyama 930
(Received May 22, 1986)

N-(1-Hydroxyalkyl)-2-imidazolidinones (**1**) were prepared by a reaction of 2-imidazolidinone with form-, acet-, propion-, and butyraldehyde. In all of these reactions, **1** were unstable and moisture-sensitive substances. The pyrolysis reaction of **1** was found to be a thermal decomposition via a condensation reaction stage after a molten state. The condensation stage obeyed 1/2- and the first-order kinetics. The kinetic data regarding the condensation reaction were evaluated by analyses of the dependences of the area of isothermal DSC curves upon the reaction time. It may be concluded that the difference provided by the reaction order and the activation parameters were caused by the number of the hydrogen atoms on the β-carbon atom adjacent to the carbon attacked the hydroxyl group of side chain in **1**. In the decomposition by electron impact of **1** and dimer of **1**, the cleavage of the five-membered ring which corresponded to the molecular-ion peak for 2-imidazolidinone (m/z 86) was considered to take place after a successive cleavage of the side chain. On the basis of both kinetic studies and ESR or Mass spectral observations, the dimerization mechanism is fully discussed.

Thermosetting resins are characterized by irreversible chemical and physical changes that take place during a "cure." The resin is polymerized into a substance of a three-dimensional network which is no longer soluble or fusible. Whenever basic studies regarding this resin or its chemical structures and curing reactions are investigated, a determination of the experimental conditions involves many difficulties. Recently, Ishida et al.[1] have a convenient method using computer simulation for the initial polymerization mechanism of the trimer (at most). However, a study regarding the reaction products and the mechanism of the thermal condensation for *N*-(1-hydroxyalkyl)-2-imidazolidinone (**1**) in the solid state has not yet been carried out.

2-Imidazolidinone (**2**) has many advantages over any other substituted ureas. Furthermore, **2** has two active imino groups similar to the amino groups of urea. **2** can not produce compounds which have an intermolecular ether formation such as uron. If **1** are cured at a certain temperature, the curing process must be similar to those of the main-chain formation for the urea resin. The present authors investigated the curing reaction of **1** under no alkaline and acid catalyst conditions by IR, ^{1}H and ^{13}C NMR measurements, as well as mass spectrum, ESR, and DSC measurements. DSC is a useful tool for measuring the thermally induced conformation transition of macromolecules[2] as well as the polymerization process. An application of DSC to the study of polymerization provides available information for a kinetic data, such as a reaction parameter. The present authors have already reported that **2**, 2-imidazolidinethione, and their *N*,*N*′-bis(hydroxymethyl) derivatives are of great value as thermally stable agents.[3] The object of the present work is divided into two parts: (1) The characterization and experimental verification of reactions related to the proposed process. (2) The condensation of the material and reaction mechanism to estimate the overall reaction for the monomer by a thermochemical analysis.

Experimental

Materials. The **2** (paraformaldehyde, ethanol, and methanol) were of reagent grade and were used without further purification. The acet-, propion-, and butyraldehyde were distilled before use.

Preparation of Samples. A preparation of *N*-(1-hydroxymethyl)-2-imidazolidinone (**1a**) (**2** 43 g(0.5 mol) and paraformaldehyde 15 g(0.5 mol)) was suspended in 25 ml of ethanol under a nitrogen atmosphere. The ethanol solution was controlled at pH 12 with a 2M†-NaOH aq soln. as the catalyst. After an elevation of the temperature by the reaction heat, the ethanol solution was cooled below 10 °C with ice. White crude crystals were filtered with suction and washed with cooled acetone in order to remove any solvents and the 2M-NaOH aq soln. A white crystal of **1a** was obtained by recrystallization from chroloform.

A preparation of *N*-(1-hydroxyethyl)-2-imidazolidinone (**1b**), *N*-(1-hydroxypropyl)-2-imidazolidinone (**1c**), and *N*-(1-hydroxybutyl)-2-imidazolidinone (**1d**) (*N*-substituted hydroxyalkyl derivatives such as **1b**, **1c**, and **1d**) were all prepared according to the reported method for monomethylolurea.[4]

Measurements. DSC and TG: A sample was heated at the rate 5 °C min^{-1} in air using a Rigakudenki TG-DSC apparatus.

IR spectrophotometry: An IR spectrum of the sample was recorded on a Nipponbunko IR-810 using the KBr-disc method.

Mass spectrum: A mass spectrum of the sample was taken with an ionization potential of between 20 and 70 eV using a JEOL-JMS-D300.

^{1}H and ^{13}C NMR measurements: **1a** and **1c** were dissolved in a deuterated dimethyl sulfoxide solution, and **1b** and **1d** in a deuterated chloroform solution, respectively. The ^{1}H and ^{13}C NMR spectra of each solution was taken on a JNM-FX-90-FT-NMR instrument.

ESR measurement: The ESR spectrum of the sample was

† 1 M=1 mol dm^{-3}.

taken under 50 and 100 kHz fields (modulation using a JEOL FE 3X spectrometer). The sample tube that fed **1c** was sealed in a vacuum system (10^{-3} mmHg (1 mmHg=133.322 Pa)) using a Hickman vacuum apparatus.

Paper chromatography: A one-dimensional paper chromatographic separation was carried out on the species using a developing solvent of 1-butanol–ethanol–water (4:1:2). The color was developed using a color-producing reagent of sodium pentacyanonitrosylferrate(III) and potassium hexacyanoferrate(III).[5]

Results and Discussion

Syntheses of 1. The physical properties of **1** are summarized in Table 1. As Table 1 shows, the observed values in the elemental analysis are in accord with the calculated values. The R_f values of the samples by paper chromatography increases upon increasing of the length of the alkyl group in the side chain. Similarly, the melting point of the sample rises upon increasing the molecular weight of **1** (except for **1d**). In the IR spectra, these samples do not show any change in the characteristic absorption due to ν_{C-H} at 2950 cm^{-1} increases with an increase in the length of the side chain. The NMR data of these samples indicate that the structure of **1** is in accord with that proposed in Scheme 1. In the mass spectra of these samples, the parent peak can be detected in the spectrum of **1a** at m/z 116. In the spectra of other samples, however, the parent peak can not be detected. The peak of $(M-H_2O)^+$ can be detected at a high intensity similar to that of the mass spectra of tertiary alcohol. The analytical and spectroscopic data regarding the structure of **1** are consistent with that proposed in Scheme 1.

Thermal Analysis. Figure 1 shows a DSC–TG curve for **1c**, as determined by a heating rate of 5 °C min^{-1}. The DSC curve exhibited two endother-

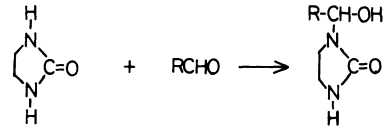

2-imidazolidinone aldehyde *N*-(1-hydroxyalkyl)-2-imidazolidinone

R: -H **1a**
-CH_3 **1b**
-CH_2CH_3 **1c**
-$(CH_2)_2CH_3$ **1d**

Scheme 1.

Table 1. Physical Properties of **1a**, **1b**, **1c**, and **1d**

		1a	**1b**	**1c**	**1d**
Elemental analysis/%	C	40.93 (41.37)[a]	45.77 (46.14)	50.06 (49.99)	53.17 (53.15)
	H	6.83 (6.94)	7.65 (7.75)	8.48 (8.39)	8.95 (8.92)
	N	24.42 (24.12)	21.52 (21.52)	19.48 (19.43)	17.65 (17.71)
Melting point (θ_m/°C)		54.5	62.5	84.5	81.0
IR spectra (cm^{-1})	ν_{NH}	3320	3340	3340	3340
	ν_{CH}	2950	2950	2950	2950
	$\nu_{C=O}$	1680	1690	1690	1690
	ν_{C-O}	1030	1100	1030	1030
R_f value[b]		0.52	0.72	0.77	0.80
Yield/%		71.3	55.1	81.7	60.5
^{1}H NMR position/ppm	In ring				
(Relative intensity:	-$(CH_2)_2$-	3.356 (4H: m)	3.458 (4H: m)	3.265 (4H: m)	3.508 (4H: m)
multiplicity)[c]	-NH	6.199 (1H: s)	5.665 (1H: s)	6.369 (1H: s)	5.780 (1H: s)
	In side chain				
	CH_3-	——	1.340 (3H: t)	0.796 (3H: t)	0.931 (3H: t)
	$(CH_3)CH_2$-	——	——	1.479 (2H: m)	1.478 (2H: m)
	-CH_2-	4.531 (2H: d)	——	——	1.478 (2H: m)
	-CH-	——	5.542 (1H: m)	4.964 (1H: m)	5.301 (1H: m)
	-OH	5.636 (1H: d)	4.773 (1H: d)	5.406 (1H: d)	4.812 (1H: d)
^{13}C NMR	In ring				
	-$(CH_2)_2$-	40.000[d]	38.298, 39.030	40.000[d]	38.274, 38.932
	-C=O	158.920	162.702	161.556	162.946
	In side chain				
	CH_3-	——	20.014	9.775	13.700
	$(CH_3)CH_2$-	——	——	27.011	18.576
	-CH_2-	66.675	——	——	35.738
	-CH-	——	72.452	76.109	75.622

a) Calculated values in parentheses. b) For paper chromatograpy. c) s: Singlet, d: doublet, t: Triplet, m: multiplet. d) Values were overlapped with the signal of DMSO-d_6.

mic peaks and an exothermic peak. The first endothermic peak is attributed to the melting point. The second endothermic peak is due to the formation of a dimer; this is confirmed by the IR, mass, and NMR spectra of samples obtained before and after the second endothermic peak (described later). The final DSC peak is found over a wide temperature range, in which the sample decomposed with the evolution of gases. The TG curve shows that the pyrolysis process for a sample takes place in two stages. In Fig. 1, the first plateau of the TG curve is probably due to a condensation of the sample to a dimer compound. The other plateau corresponds to a thermal degradation and a decomposition reaction. The kinetic consideration is carried out by this condensation. First, the present authors discuss the kinetic analysis using for an example McGhie method.[6] The DSC measurements are carried out by the method in which the sample was hermetically sealed in an aluminum pan and in a DSC cell using an isothermal mode. Condensation was studied in the temperature range of 90—150 °C. Figure 2 shows typical isothermal condensation curves for **1c**. After an induction period, during which condensation occurred at a slow rate, there was a rapid increase in the endothermic heat of the condensation region (apparently obeying 1/2- and first-order kinetics). By calling the representative total area under a given isothermal curve a, and the fractional area up to the time t, x, the 1/2- and the first-order kinetics plots of $2\times[a^{1/2}-(a-x)^{1/2}]$ and $\ln[a/(a-x)]$ vs. $t-t_0$ for each curve are linear. Figures 3 and 4 show these plots for the isothermal condensation of four samples at any temperature. The data was normalized with respect to time by plotting the time after the induction period t_0. Thus, each isothermal curve yielded two important quantities, t_0 and k. The 1/2- and the first- order rate constant was obtained from the slope of the curve in Figs. 3 and 4. The rate constant for the condensation of **1** is summarized in Table 2. Second, Arrhenius plots are shown in Fig. 5. The activation energy was obtained by the slope and the frequency factor was obtained by the intercept of these lines (Fig. 5). The results of these calculations are summarized in Table 3. The reaction order of **1a** is different from the other three samples. **1b** has an activation energy about half that of **1c** or **1d** and **1b** has an activation entropy about two-times that of **1c** or **1d**. **1c** has an activation energy and the activation entropy that are the same order as **1d**. It can be assumed that the difference provided by the reaction order and the

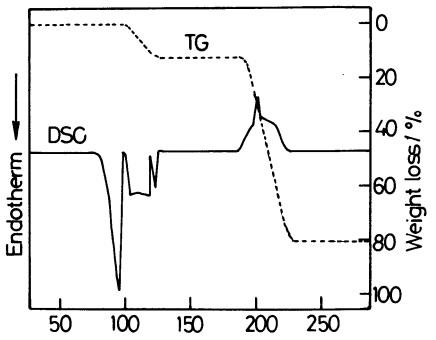

Fig. 1. DSC and TG curves of **1c**.

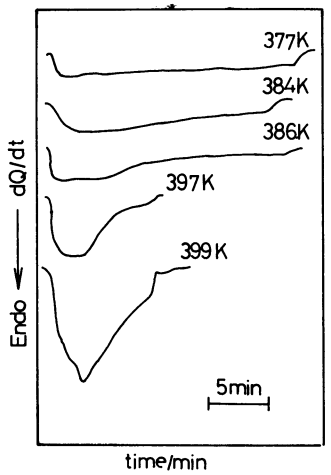

Fig. 2. Isothermal polycondensation DSC curves for **1c**.

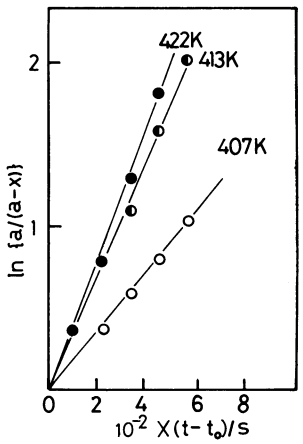

Fig. 3. First order kinetic plots of $\ln[a/(a-x)]$ vs. $t-t_0$ for the isothermal polycondensation of **1a**.

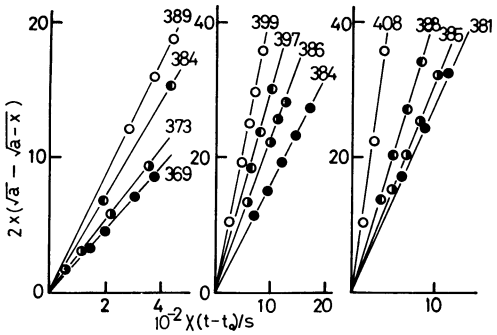

Fig. 4. 1/2 order kinetic plots of $2\times[a^{1/2}-(a-x)^{1/2}]$ vs. $t-t_0$ for the isothermal polycondensation of **1b**, **1c**, **1d**.

activation parameters is caused by the number of the hydrogen atom (β-hydrogen atom) on β-carbon atom adjacent to the carbon attached to the hydroxyl group of the side chain in **1**. These compounds may be grouped, therefore, into three general classes: (1) no β-hydrogen atom (**1a**); (2) three β-hydrogen atoms (**1b**) and (3) two β-hydrogen atoms (**1c**, **1d**).

Thermal Condensation of 1. The TG analysis shows that a dehydration of the samples can be expected for the thermal condensation of **1** since the weight loss of the first plateau at the temperature range of the condensation corresponds to that of about one mole of water. The IR spectra of the condensation products show that the absorption due to ν_{C-O} at 1030 cm^{-1} decreases in intensity (Fig. 6). The ^{13}C NMR spectra of **1c** and its condensation product is given as an example in Fig. 7. This figure shows that the signal at δ 161.556 due to the carbonyl group separates into two signals, and the signal due to the α-carbon atom attached to the hydroxyl group splits after condensation. These results show that the formation process of dimer seemed to be dehydrated as intermolecular combination (Scheme 2). The mass spectra of the condensation products also support this dimer formation. The mass spectra of the condensation products are summarized in Table 4. In this Table 4 **1a**-H, **1b**-H, **1c**-H, and **1d**-H are used for symboliz-

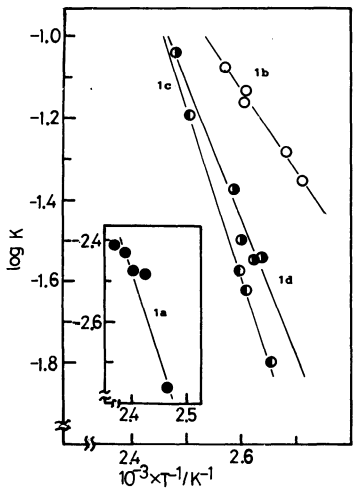

Fig. 5. Arrehnius plots of the first order rate constants for the polycondensation of **1a**, and 1/2 order for the polycondensation of **1b**, **1c**, and **1d**.

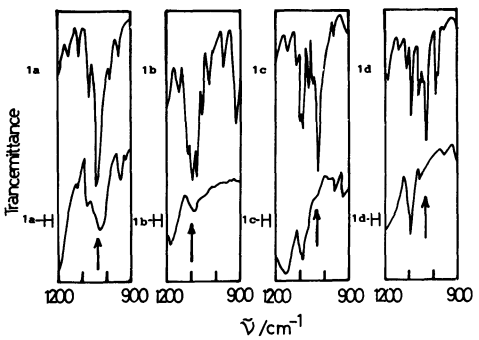

Fig. 6. Change of ν_{C-O} absorption on IR spectra of *N*-hydroxyalkyl derivatives.

Table 2. Reaction Rate for the Condensation of **1**

Compound	Temp/K	Reaction order	Rate constant[a)]
	407		1.72×10^{-3}
	413		3.34×10^{-3}
1a	416	1.0	3.36×10^{-3}
	419		3.72×10^{-3}
	422		3.84×10^{-3}
	369		4.39×10^{-2}
	373		5.15×10^{-2}
1b	383	0.5	7.09×10^{-2}
	384		7.37×10^{-2}
	389		8.52×10^{-2}
	377		1.62×10^{-2}
	384		2.37×10^{-2}
1c	386	0.5	2.78×10^{-2}
	397		5.70×10^{-2}
	399		6.51×10^{-2}
	381		2.85×10^{-2}
	382		2.87×10^{-2}
1d	385	0.5	3.13×10^{-2}
	388		4.23×10^{-2}
	408		9.30×10^{-2}

a) Unit in 1.0(reaction order); s^{-1}. Unit in 0.5; $mol^{1/2}$ $l^{-1/2}$ s^{-1}.

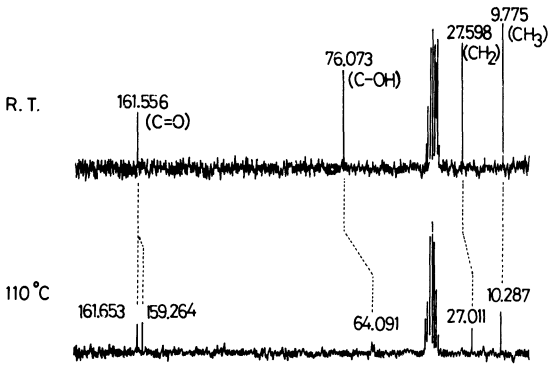

Fig. 7. ^{13}C NMR spectra of **1c** and **1c**–H.

Table 3. Kinetic Data for the Condensation of **1**

Compound	A[a)]	ΔE_a / kJ mol^{-1}	ΔS^* / e.u.
1a	3.98×10^{7}	8.07	−26.40
1b	1.65×10^{4}	39.37	−41.65
1c	2.16×10^{9}	80.46	−18.24
1d	1.59×10^{8}	71.30	−23.43

a) Unit in **1a**: s^{-1}, Unit in **1b**, **1c**, and **1d**: $mol^{1/2}$ $l^{-1/2}$ s^{-1}.

ing the thermal condensation products of **1a**, **1b**, **1c**, and **1d**, respectively. There are no peaks due to trimer or oligomer in these mass spectra. The observed fragment ions in the mass spectra of the condensation products support the main fragmentation mechanism of the dimer by the typical representative **1c** (Fig. 8). The amount of aldehyde liberated during the thermal reaction of **1** was about 10% (in quantities of the sample fed with the flask). The elimination of the corresponding aldehyde due to the pyrolysis of **1** is a reverse reaction of *N*-hydroxyalkylation. Consequently, the pyrolysis of **1** leads to the production of **2** (10% of the amount of the samples fed with the flask). A

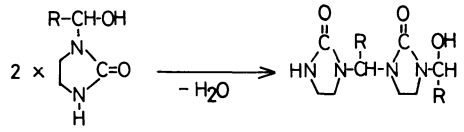

Scheme 2.

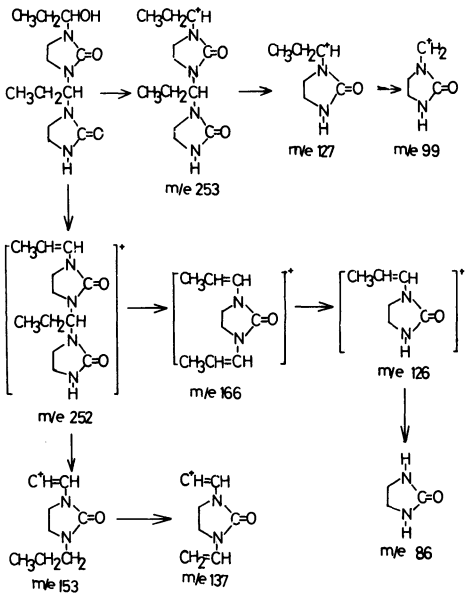

Fig. 8. Main fragmentation for **1c**–H.

Table 4. Mass Spectral Data for **1a**-H, **1b**-H, **1c**-H, and **1d**-H

m/z	Relative intensity[a]	Observed molecular weight	U.S.[c]	Probable ion composition
(I) **1a**-H				
86.0	43.60	86.0498 (86.0932)[b]	2.0	$C_3H_6N_2O$
99.0	100.00	99.0557 (99.1121)	2.5	$C_4H_7N_2O$
113.0	12.96	113.0650 (113.1389)	2.5	$C_5H_9N_2O$
183.0	15.60	183.0802 (183.1895)	4.5	$C_7H_{11}N_4O_2$
196.0	4.80	196.1038 (196.2084)	5.0	$C_8H_{12}N_4O_2$
(II) **1b**-H				
86.0	100.00	86.0496 (86.0932)	2.0	$C_3H_6N_2O$
112.0	21.83	112.0630 (112.1310)	3.0	$C_5H_8N_2O$
113.0	1.61	113.0633 (113.1381)	2.5	$C_5H_9N_2O$
138.0	4.89	138.0819 (138.1688)	4.0	$C_7H_{10}N_2O$
139.0	0.81	139.0844 (139.1716)	3.5	$C_7H_{11}N_2O$
(III) **1c**-H				
86.0	32.20	86.0295 (86.0932)	2.0	$C_3H_6N_2O$
99.0	6.55	99.0645 (99.1121)	2.5	$C_4H_7N_2O$
126.0	55.41	126.0771 (126.1578)	3.0	$C_6H_{10}N_2O$
127.0	100.00	127.0845 (127.1657)	2.5	$C_6H_{11}N_2O$
137.0	4.94	137.0797 (137.1609)	4.5	$C_7H_9N_2O$
153.0	1.36	153.1029 (153.2035)	3.5	$C_8H_{13}N_2O$
166.0	6.49	166.1119 (166.2224)	4.0	$C_9H_{14}N_2O$
252.0	1.99	252.1603 (252.3156)	5.0	$C_{12}H_{20}N_2O_2$
253.0	0.34	253.1727 (253.3235)	4.5	$C_{12}H_{21}N_2O_2$
(IV) **1d**-H				
86.0	67.87	86.0295 (86.0932)	2.0	$C_3H_6N_2O$
99 0	6.43	99.0569 (99.1121)	2.5	$C_4H_7N_2O$
125.0	100.00	125.0719 (125.1499)	3.5	$C_6H_9N_2O$
139.0	6.46	139.0829 (139.1716)	3.5	$C_7H_{11}N_2O$
153.0	2.73	153.1009 (153.2035)	3.5	$C_8H_{13}N_2O$
165.0	13.67	165.0997 (165.2145)	4.5	$C_9H_{13}N_2O$
179.0	14.62	179.1192 (179.2413)	4.5	$C_{10}H_{15}N_2O$
194.0	2.66	194.1424 (194.2760)	4.5	$C_{11}H_{17}N_2O$

a) Relative intensity referred to base peak of spectrum as 100. b) Calculated values. c) U.S.=Degree of unsaturation.

separation of the various mixtures into the liberated **2** could not be verified. Thus, the observed values through elemental analyses are not in full agreement with calculated ones.

Reaction Mechanism for Thermal Condensation in Solid State. Dimerization of **1a**: **1a** has a γ-lactam structure. Therefore, **1a** shows a "tautomeric change" as shown in Scheme 3. In the DSC measurement over the high-temperature range, it is expected that an activated complex is formed from two molecules of the lactim (enol isomer) of **1a** (Scheme 4). These equilibrium conditions for Scheme 4 lie far to the right, showing the reaction process during a smooth formation of the activation complex. At this equilibrium, therefore, the reaction for dimerization apparently obeys first-order kinetics. The expected process for the dimerization of **1a** is as follows.

The reaction mechanism for the dimerization of **1b**, **1c**, and **1d**: As described in the previous section, the dimerization of **1** shows first-order kinetics, whereas in **1b**, **1c**, and **1d**, the order of reaction is to the 1/2 order. It is expected that the dimerization of **1b**, **1c**, and **1d** proceeds by the same mechanism. The use of the results of ESR and mass spectra clarifies the difference in the order of the reaction. ESR measurements were carried out for **1c** at room temperature, 70, 100, 130, and 150 °C. **1c** was in a solid state at room temperature and at other temperatures melted. As Fig. 9 shows, the signal may be due to an intermediate material which participates in the thermal condensation, since this signal was observed alone at the temperature range of the thermal-condensation process. It shows that the intermediate material is considered to form at the pertinent temperature range (70—130 °C). Also, this signal deviates from 0 G to a low magnetic field, and shows a discernible shoulder at the low-magnetic-field side of the main signal. The above results do not indicate that **1c** thermally polymerizes to form the radical. Therefore, the present authors conclude that **1c** in this system forms the electron-transfer complex. After the ESR measurement of **1c** (at 100 °C), the sample tube fed with **1c** was cooled to room temperature. During the ESR measurement under these conditions, the same signal (observed at 100 °C) was reproduced in the ESR spectrum of this sample. This result seems to show that the thermal condensation stops and the resulting activity species remain unaltered. This behavior resembles ordinary very closely living polymerization regarding chemical properties. The possible structure of intermediates formed during the activated state in the course of the dimerization process for **1b**, **1c**, and **1d** is the activated complex (A) and the enol type (B) like lactim (Scheme 5).

The presence of (A) was confirmed by the ESR measurements, and (B) gave no direct evidence concering its existence in the solid state. In the melted state, however, the presence of (B) have likewise been formed in the case of cyanuric acid. By a comparison of structures (A) and (B), the hydroxyl group of (A) was easier to eliminate than that of (B). In the next step, the activated complex (C) (Scheme 5) was formed

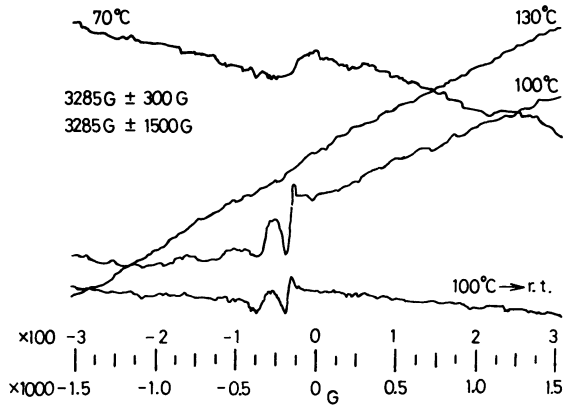

Fig. 9. ESR spectra of **1c**.

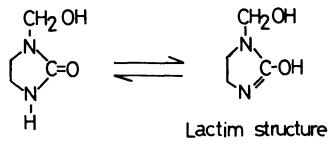

Scheme 3.

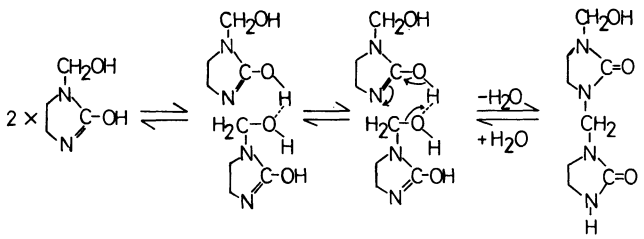

Scheme 4.

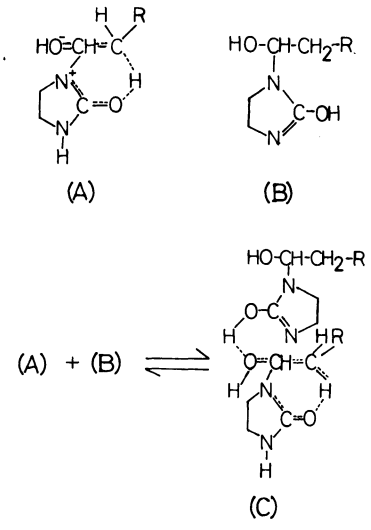

Scheme 5.

from (A) and (B). Now, on the assumption that the overall reaction of dimerization of **1** proceeds with the apparent first-order reaction (such as the dimerization of **1a**), the main conclusion to be drawn from these results is as follows. The concentration of **1**, (A), (B), and (C) are symbolized as [M], [A], [B], and [C], respectively. The equation for each process is as follows:

For the formation of (A)

$$M \rightleftharpoons A \qquad K_1[M] = [A]. \tag{1}$$

For the formation of (B)

$$M \rightleftharpoons B \qquad K_2[M] = [B]. \tag{2}$$

For the formation of (C)

$$A + B \rightleftharpoons C \qquad K_3[A][B] = [C], \tag{3}$$

where K_1, K_2, and K_3 are the equilibrium constants for each process. If the values of [A] and [B] in Eq. 3 are replaced by the corresponding expressions as Eqs. 1 and 2, it is found that

$$K_1 \cdot K_2 \cdot K_3[M]^2 = [C]. \tag{4}$$

According to the previous assumption, for an overall reaction,

$$\text{Reaction rate} = k_0[M], \tag{5}$$

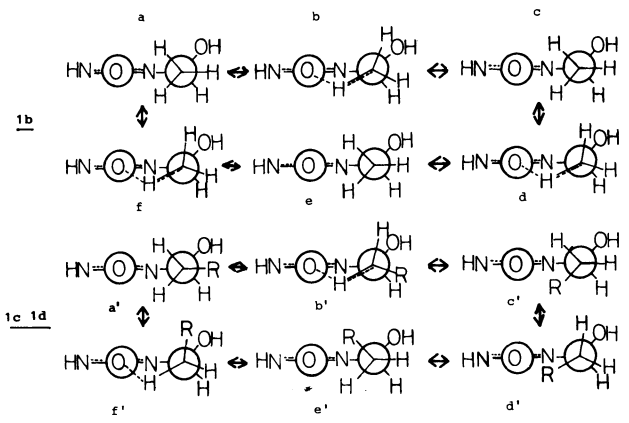

Fig. 10. Conformations of **1b**, **1c**, and **1d**.

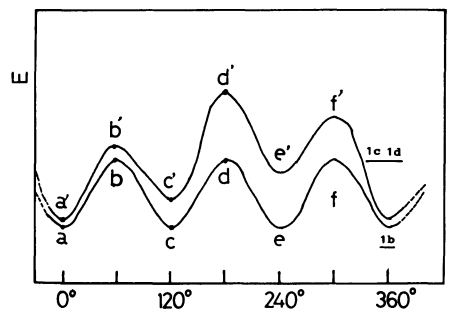

Fig. 11. Rotational energy profiles for **1b**, **1c**, and **1d**.

where k_0 is the rate constant for the overall reaction. When the value of [M] in Eq. 4 is substituted into Eq. 5,

$$\text{Reaction rate} = k_0\{1/(K_1 \cdot K_2 \cdot K_3)\}^{1/2}[C]^{1/2}. \tag{6}$$

When $k_0\{1/(K_1 \cdot K_2 \cdot K_3)\}^{1/2}$ is substituted for k, Eq. 6 becomes

$$\text{Reaction rate} = k[C]^{1/2}. \tag{7}$$

Equation 7 shows that the reaction for the dimerization of **1b**, **1c**, and **1d** proceeds by a 1/2-order reaction. This result agrees with those of the DSC measurements. It is expected for **1b**, **1c**, and **1d** that the DSC measurement was taken in order to obtain information regarding the formation of (C) to the dimer. From these results, it is clear that (A), (B), and (C) are formed during the induction period. The effect of the number of β-hydrogen atoms on the activation parameters must be discussed. **1c** and **1d** have methyl and ethyl groups on the β-carbon atom, respectively. The difference in the activation parameters between **1c** and **1d** for the dimerization is negligibly small. Therefore, the effect of these alkyl groups as the electron donor on the electron-transfer complex (A) is negligible. Figure 10 shows conformations of **1b**, and **1c** and **1d** which are concerned with a rotation about the bond between the α- and the β-carbon atoms attached to the hydroxyl group. Their interconversion processes are represented by the Newman projection formulae. The formation of the electron-transfer complex in the case of **1b** is formed at b, d, and f (Fig. 10). However, in the case of **1c** and **1d**, the formation of the electron-transfer complex is formed at b′ and f′. The formation of (A) at b, b′, d, f, and f′ should be unstable forms owing to their eclipsed geometries. This is the reason for the formation of (A), which is only at the pertinent temperature range (as shown in the ESR spectra). Figure 11 shows the rotational-energy profiles for **1b**, **1c**, and **1d**. According to these profiles, it is definite in the case of **1c** and **1d** that the rotational-energy of structures b′ and f′ is higher than that for b and f in **1b**. This is the reason for the difference in the activation parameters between **1b** and **1c** or **1d**.

We acknowledge the good advice of Prof. Eiichi Tsukurimichi and Dr. Toshiaki Yoshimura. We thank Mr. Yoshiharu Yoneyama for NMR measurements and Miss Misao Shinoda for the Mass spectra. We thank Prof. Shigeya Takeuchi for good advice regarding DSC measurement.

References

1) S. Ishida, *Netsukokaseijushi*, **1**, 40 (1980).
2) Y. Fujita and Y. Noda, *Bull. Chem. Soc. Jpn.*, **57**, 2177 (1984).

3) C. Shimasaki, A. Uchida, H. Oonishi, Y. Iwai, and M. Wakabayashi, *Nippon Kagaku Kaishi*, **1983**, 1761.
4) S. Takeuchi, "Yukikagobutsugoseiho," ed by Yukigosei Kagakukyokai, Gihodo, (1969), pp. 27, 61.
5) M.Takimoto and K. Koeda, *Kogyo Kagaku Zasshi*, **63**, 797 (1960).
6) A. R. McGhie, P. S. Kalyanaraman, and A. F. Garito, *J. Polym. Sci., Polym. Lett. Ed.*, **16**, 335 (1978).